

A miniaturized dual-band planar antenna with a square ring defected ground structure for 5G millimetre-wave applications

Mamadou Mamarou Diallo¹, Dominic Bernard Onyango Konditi², Olivier Videme Bossou³

¹Department of Electrical Engineering (Telecommunication Option), Pan African University,
Institute for Basic Sciences Technology and Innovation (PAUSTI), Nairobi, Kenya

²School of Electrical and Electronics Engineering, Technical University of Kenya (TUK), Nairobi, Kenya

³Department of Electrical Engineering and Telecommunications, National Advanced School of Engineering, University of Yaoundé I,
Yaoundé, Cameroon

Article Info

Article history:

Received Jun 4, 2022

Revised Aug 26, 2022

Accepted Sep 9, 2022

Keywords:

5G

Dual-band

Microstrip antenna

Mm-wave

Square ring defected ground structure

ABSTRACT

The high demand for wireless wideband services has led to evolving of a new mobile network standard, which is known as '5G'. For 5G to meet the essentials in terms of bandwidth, the industry should leverage the mm-Wave band (24-300 GHz). Further, miniaturized antennas that operate in multiple frequency bands are required for future space-constrained devices. In this manuscript, a compact dual-band circular microstrip antenna which has a square ring defected ground structure (SR-DGS) is investigated for 5G mobile systems. The design is accomplished using Ansys-HFSS 2021R1. The Rogers RT/duroid (5880) substrate, which has a permittivity of 2.2, a tangent loss of 0.0009, and a thickness of 1.575 mm, is used as a dielectric material. The antenna has physical dimensions of $5 \times 4 \times 1.575$ mm³ with an electrical size of $0.458\lambda_0 \times 0.366\lambda_0 \times 0.144\lambda_0$; λ_0 represents the wavelength in free space at 27.50 GHz. Impedance bandwidths of 1.34 GHz (27.50 GHz-28.84 GHz) and 2.26 GHz (37.74 GHz-40 GHz) are achieved at the 28 GHz and 38 GHz bands, respectively. The antenna resonates at 28.1875 GHz and 38.5625 GHz with respective gains of 7.2 dB and 7.65 dB. The proposed antenna is a promising candidate for 5G communications due to its miniaturized size.

This is an open access article under the [CC BY-SA](https://creativecommons.org/licenses/by-sa/4.0/) license.



Corresponding Author:

Mamadou Mamarou Diallo

Department of Electrical Engineering (Telecommunication Option), Pan African University

Institute for basic Sciences, Technology and Innovation (PAUSTI)

Nairobi, Kenya

Email: mamarou.mamadou@students.jkuat.ac.ke

1. INTRODUCTION

The proliferation of mobile phone users along with the integration of new services on the internet have led both the industry and the research community to evolve a new standard to support data-hungry services. The current 4G mobile communication standard cannot support services like the internet of things (IoT), vehicle-to-vehicle (V2V) communications, smart cities, and telemedicine because it does not provide the required bandwidth for such applications. To overcome the limitation of bandwidth and latency of 4G, 5G is being developed. For 5G to meet the requirements of future wireless communication systems, it should provide larger bandwidth, higher gains, and low latency [1].

The US federal communications commission (FCC) and other advanced countries have reserved two frequency ranges (FRs) for 5G implementation. The FRs are the mid-band commonly known as the sub-6 GHz band (1 GHz-6 GHz) and the millimeter-wave (mm-Wave) band (24-300 GHz) [2]. Several applications, such as the wireless local area network (WLAN), the worldwide interoperability for microwave access (WiMAX), and

the current long-term evolution (LTE), have already jammed the previous band (FR1). As a result, the FR1 band is unable to meet the vast bandwidth requirement for 5G. On the other hand, the latter band (FR2) provides many unused frequencies and can support several applications with a low risk of interference.

Planar antennas are the most suited for dual or multi-band applications due to their low profile, lightweight, low cost of fabrication, and ease of integration in space-constrained devices [3]. In the last few decades, several planar antennas for WLAN, LTE/4G, WiMAX, and 5G applications have been investigated in the open literature. Different Microstrip antenna shapes, including Heart-shaped [3], rectangular [4], circular shapes [5]-[7]; Dolly-shaped [8], and Rho-shaped [9], along with dual-band techniques such as defected ground structures (DGS), slots or slits etching and Metamaterials have been investigated. A circular patch antenna for 5G applications to compare two feeding techniques, namely, coaxial probe and Microstrip line is designed in [10]. The mono-band patch antenna resonated at 28 GHz with bandwidths of 0.792 GHz and 0.660 GHz for the coaxial probe and Microstrip line, respectively. Similarly, a single patch antenna for 5G applications that operates at 28 GHz is reported in reference [11]. The antenna consists of an inverted C-shape with overall dimensions of $12 \times 15 \times 0.508 \text{ mm}^3$, a bandwidth of 1.23 GHz, and a gain of 7.4 dB. In the same idea, a conventional rectangular Microstrip single antenna for 5G mm-Wave communications is reported in [12]. To improve the radiation parameters of the antenna, slots are inserted in the patch area. The results showed an overall antenna size of $7 \times 7 \text{ mm}^2$, a bandwidth of 2.48 GHz (26.8116-29.2897 GHz), and a peak gain of 6.34 dB. An inset-fed rectangular Microstrip antenna that resonates at 28 GHz is investigated in [13]. The calculated dimensions of the antenna are optimized using FEKO software to achieve a large bandwidth of 5.57GHz with a compact size of $6.2 \times 8.4 \times 1.57 \text{ mm}^3$. Paul *et al.* [14] proposed a 5G wideband rectangular Microstrip antenna with partial ground plane. A bandwidth of 2.567 GHz (26.984-29.551 GHz) with an overall size of $20 \times 17 \times 1.575 \text{ mm}^3$ is achieved. To improve the performance of the designed antenna, an isoscele triangular shape is cut on the left side of the patch. The final design provided a gain of 8.39 dB. It can be noticed that better performance is achieved in the works investigated [10]-[14]. However, these studies have limitations in the sense that they did not consider multi-band capabilities, which is crucial for antennas to support several applications.

To achieve the multi-band and wideband characteristics, researchers have devised several techniques including DGS, slots or slits etching, metamaterials (MM), and multiple antennas with different resonant frequencies. Qayyum *et al.* [15] studied a dual-band patch antenna with a circular ring DGS for 5G mm-Wave applications resonating at 28 GHz and 38 GHz. The overall size of the antenna element is $7.23 \times 7.23 \times 0.6 \text{ mm}^3$ with impedance bandwidths of 0.87 GHz and 1.07 GHz at 28 GHz and 38 GHz, respectively. In the same line, a compact dual-band (28 GHz and 38 GHz) with a rectangular DGS is illustrated in [16] for 5G communications. Bandwidths of 0.7 GHz and 0.5 GHz are achieved at 28 GHz and 38 GHz, respectively with antenna electrical dimensions of $(1.12 \times 1.31 \times 0.035) \lambda_0$.

Furthermore, an elliptically slotted semi-circular patch radiator (ESSPR) with a DGS, which has a wideband performance for 5G devices is reported in reference [17]. Although the antenna exhibits a large bandwidth of 2.14 GHz in the sub-6 GHz band, its size of $23.885 \times 23.885 \times 1.405 \text{ mm}^3$ is too large for space-limited applications. The double bands patch antenna for 5G handheld devices presented in [18] consists of two antennas. The first radiator, which is directly fed by the microstrip line, resonates at the lower band (38 GHz). The second patch is then excited by the first patch to resonate at the upper band (60 GHz). A tri-band umbrella-shaped antenna for 5G mm-Wave applications is illustrated in reference [19]. The radiator resonated at 28 GHz, 38 GHz, and 55 GHz with gains of 6.6 dB, 7 dB, and 7.35 dB respectively. In addition, a dual-band (26 GHz and 28 GHz) microstrip antenna for 5G is shown in [20]. The dual-band in this work is achieved by inserting two symmetrical L-shaped slots and a centered square slot on the conductor. The overall dimensions of the proposed antenna are $20 \times 16.5 \times 0.508 \text{ mm}^3$. The simulated result stipulated bandwidths of 0.55 GHz/1.1 GHz and gains of 8.63 dB/11.26 dB at 26 GHz and 28 GHz, respectively. Moreover Mpele *et al.* [21] illustrates a compact dual-band elliptical patch antenna with a coplanar waveguide for 5G applications. The proposed design in this article is composed of two dielectric substrates superposed to each other. The parameters are optimized by inserting two inverted F-shaped slots on the ground. The antenna resonates at 28 GHz and 38 GHz with respective bandwidths of 4.51 GHz and 4.26 GHz.

In this work, a miniaturized dual-band circular microstrip antenna with a square ring defected ground structure (SR-DGS) is investigated. Our proposed antenna operates in the mm-Wave band (28 GHz/38 GHz) for 5G applications. These particular frequencies were chosen due to their low atmospheric absorption. The novelty of the SR-DGS antenna is its miniaturized size compared to the existing designs, which makes it one of the most promising candidates for space-constrained applications.

The rest of the manuscript is organized as follows: In section 2, the design method and procedure are illustrated. The results and discussions are presented in section 3. Finally, section 4 concludes this work.

2. ANTENNA DESIGN

A miniaturized dual-band circular microstrip patch antenna for 5G mobile communications is presented in this work. Ansys-HFSS 2021R1, a high-frequency structure simulator that is available commercially and is based on the finite element full-wave analysis Method, is used to simulate the model (FEM). Between the patch and the ground plane, a Rogers RT/duroid 5880 substrate with a dielectric constant of 2.2, a tangent loss of 0.0009, and a thickness of 1.575 mm is utilized. The Rogers RT/duroid 5880 material was selected because it is known to provide better performance due to its low dielectric constant. Initially, the radius of the patch is determined using (1) and (2) [22]. The summary of the initial values is provided in Table 1. In the next step, a parametric analysis of dimensions namely the radius of the patch, the length, and the width of the dielectric material is performed to achieve the desired performance. The optimized parameters for the final design are presented in Table 2. Finally, a square ring (SR) slot commonly known as a defected ground structure (DGS) is etched on the ground to achieve the desired resonant frequencies and to reduce the return loss. The layout of the final design is illustrated in Figure 1. The top, bottom, and side views of the antenna are shown in Figures 1(a)-(c) respectively.

$$R_p = \frac{F}{\sqrt{1 + \frac{2h}{\pi \epsilon_r F} \left[\ln\left(\frac{F\pi}{2h}\right) + 1.7726 \right]}} \tag{1}$$

Where $F = \frac{8.79 \times 10^9}{f_r \sqrt{\epsilon_r}}$ (2)

R_p =the radius of the patch (cm), f_r is the resonant frequency (Hz), ϵ_r is the dielectric constant, and h is the height of the dielectric material in centimeters (cm).

Table 1. Summary of the initial values

Parameters	Symbols	Values (mm)
Radius of the Patch	R_p	1.2159
Height of the patch	H_p	0.035
Length of the substrate	L_s	7
Width of the substrate	W_s	6
Length of the ground plane	L_g	7
Width of the ground plane	W_g	6
Length of the feedline	L_f	1.54
Width of the feedline	W_f	1
Height of the substrate	H_s	1.575

Table 2. Summary of the optimized values

Parameters	Symbols	Values (mm)
Radius of the Patch	R_p	1.6
Height of the patch	H_p	0.035
Length of the substrate	L_s	5
Width of the substrate	W_s	4
Length of the ground plane	L_g	5
Width of the ground plane	W_g	4
Length of the feedline	L_f	1.54
Width of the feedline	W_f	0.75
Height of the substrate	H_s	1.575
Width of the SRS	b	0.8

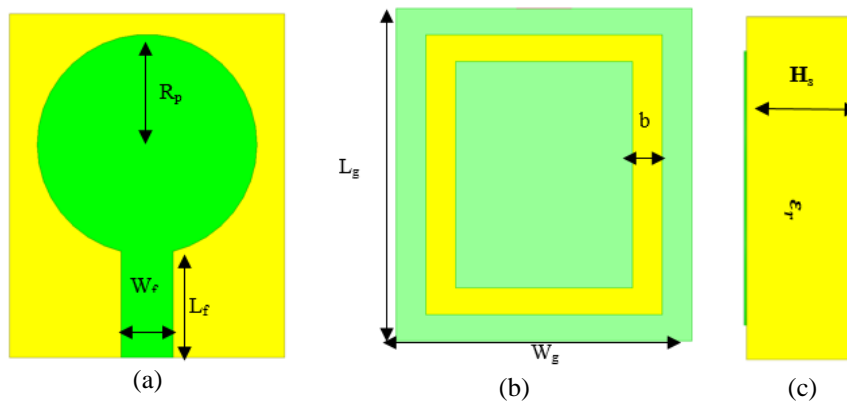


Figure 1. Design layout, (a) top view, (b) bottom view, and (c) side view

The patch area of the antenna, which describes the compactness of the antenna, is calculated using (3).

$$A_p = \pi R_p^2 + L_f \times W_f \tag{3}$$

$$A_p = (1.6)^2 * \pi + 1.54 * 0.75 = 9.19 \text{ mm}^2$$

Where R_p = radius of the patch, L_f = length of the feedline, W_f = the width of the feedline.

2.1. Effect of the square ring defected ground structure (SR-DGS)

After the circular microstrip antenna is simulated using the software, a square ring (SR) slot, which is commonly known as a DGS is cut on the ground plane to achieve better performance of the antenna. Figure 2 shows the effect of the SR-DGS on the reflection coefficient Figure 2(a), gain Figure 2(b), and VSWR Figure 2(c). It was observed that the SR-DGS not only shifted the resonant frequencies at the desired points, but also positively affected the antenna performance such as the reflection coefficient, gain, and VSWR. In addition, the structure (SR-DGS) has reduced the lower resonant frequency by about 2.80%, which demonstrates that the proposed antenna is miniaturized.

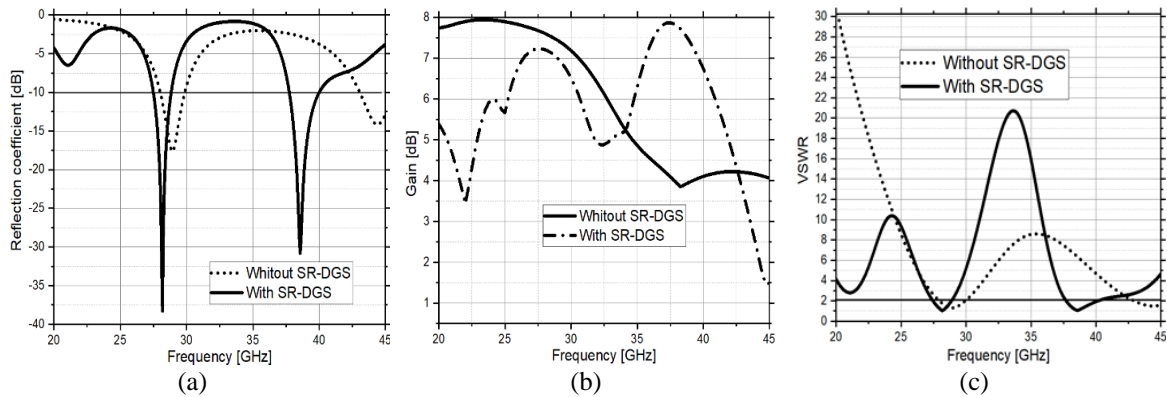


Figure 2. Effect of the SR-DGS, (a) reflection coefficient, (b) 2D Gain, and (c) VSWR

2.2. Parametric analysis

In this sub-section, the effect of the width of the SR-DGS (b) is analyzed. The values of the width considered in the analysis are $b = 0.4$ mm, 0.8 mm, and 1.2 mm. The result is shown in Figure 3. It can be observed that as the width of the ring varies, so do the parameters of the antenna. The resonant frequencies move toward the right as the width of the square ring increases. The best performance in terms of reflection coefficient Figure 3(a), VSWR Figure 3(b), bandwidth, and the desired resonant frequency is achieved at $b = 0.8$ mm.

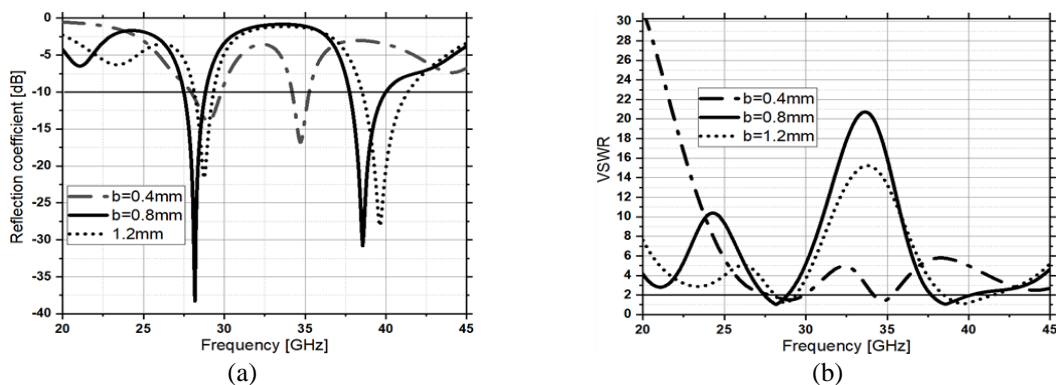


Figure 3. Parametric analysis, (a) Reflection coefficient and (b) VSWR

3. RESULTS AND DISCUSSIONS

A microstrip radiator's primary performance indicator can be roughly divided into two categories: The impedance and properties of radiation. The reflection coefficient, return loss (dB), and voltage standing wave ratio are used to evaluate the former, which specifies how the transmission line is matched to the radiator (VSWR). The latter describes the antenna's radiation characteristics. The far-field gain, radiation efficiency, directivity, and polarization are used to gauge the radiation [23]. In this section, the listed parameters are discussed.

3.1. Return loss, Bandwidth, VSWR, and Gain

The antenna parameters such as the radiation efficiency, reflection coefficient, and VSWR are given in Figure 4. It can be observed from Figure 4(a) that the -10 dB impedance bandwidths are 1.34 GHz (27.50 GHz-28.84 GHz) and 2.26 GHz (37.74 GHz-40 GHz). The antenna resonates at 28.1875 GHz and 38.5625 GHz with reflection coefficients of -38.3 dB and -30.8 dB, respectively.

In addition, the radiation efficiency is shown in Figure 4(b) is greater than 94% throughout the frequency range. The voltage standing wave ratio (VSWR), which describes the impedance matching between the load and the transmission line, is presented in Figure 4(c). The VSWR values are 1.0175 and 1.0580 at the resonant frequencies, respectively. Antenna parameters as shown in Figure 5. Moreover, the axial ratio in Figure 5(a) demonstrates that the proposed antenna is linearly polarized since this ratio is greater than 3 dB in the entire frequency range. Similarly, the gain versus frequency is presented in Figure 5(b). Peak gains of 7.2 dB and 7.65 dB are observed at the two resonant frequencies, respectively.

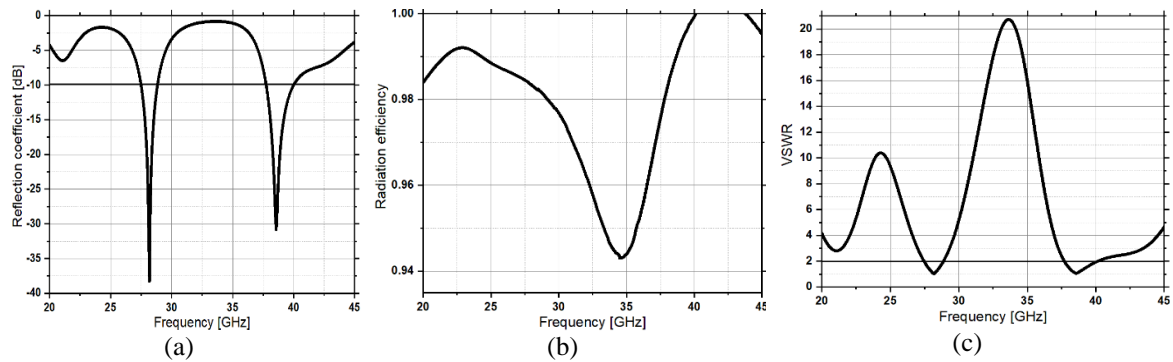


Figure 4. Antenna parameters, (a) reflection coefficient, (b) radiation efficiency, and (c) VSWR

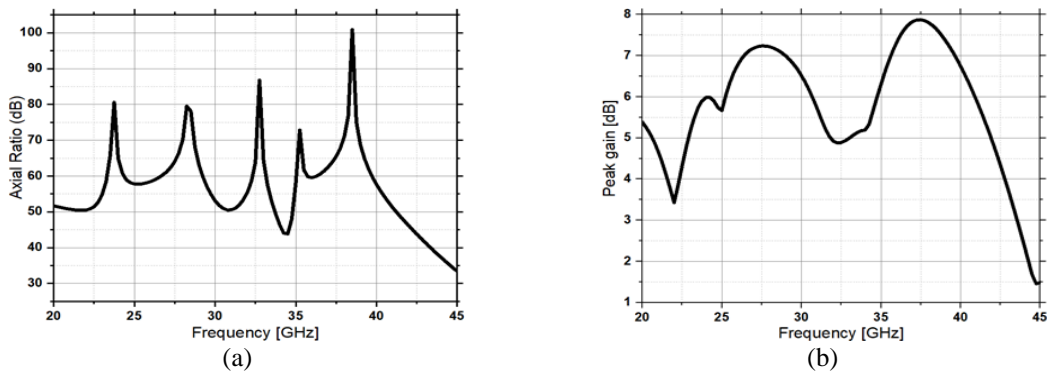


Figure 5. Antenna parameters, (a) axial ratio and (b) gain 2D plot

3.2. Current distribution

In this section, the current distribution on the antenna element is discussed. Figure 6 shows the current flows on the radiating element. It can be noticed that, at 28.1875 GHz, the current is denser at the left and right side edges of the patch with a maximum current of 4.7866 [A/m] as shown in Figure 6(a). On the contrary, less current is distributed at the center of the circle and, in the middle of the feedline. At the second resonant frequency (38.5625 GHz), the maximum current value of 4.8668 [A/m] is observed at the feedline Figure 6(b). The current is also distributed at the extremities of the patch with the lowest current at the top part of the circle.

3.3. Radiation pattern

The radiation pattern is defined as the graphical representation of the emission and reception of the wave front at the antenna. In other words, it provides the representation of the strength of the transmitted or received signal in various directions. The polar plot of the radiation patterns in the E-plane ($\phi=0$ deg.) and H-plane ($\phi=90$ deg.) are given in Figure 7 and Figure 8, respectively for the frequencies of 28 GHz and 38 GHz. It can be noticed from Figure 7(a) and Figure 7(b) that, the cross-polarization at both frequencies provided quasi-omnidirectional radiation, while some nulls can be seen in the co-polarization.

On the other hand, from Figure 8(a) and Figure 8(b), the co-polarization patterns stipulate quasi-omnidirectional radiation, and the cross-polarization patterns present bi-directional radiation at both frequencies (28 GHz, 38 GHz). Furthermore, to show the effectiveness of our work, the proposed work is compared with some designs found in the open literature. The comparison is presented in Table 3. The key performance indexes considered in the comparison include the frequency bands, the -10 dB impedance bandwidth, the gain, the voltage standing wave ratio (VSWR), the electrical dimensions, and the bandwidth dimension ratio (BDR).

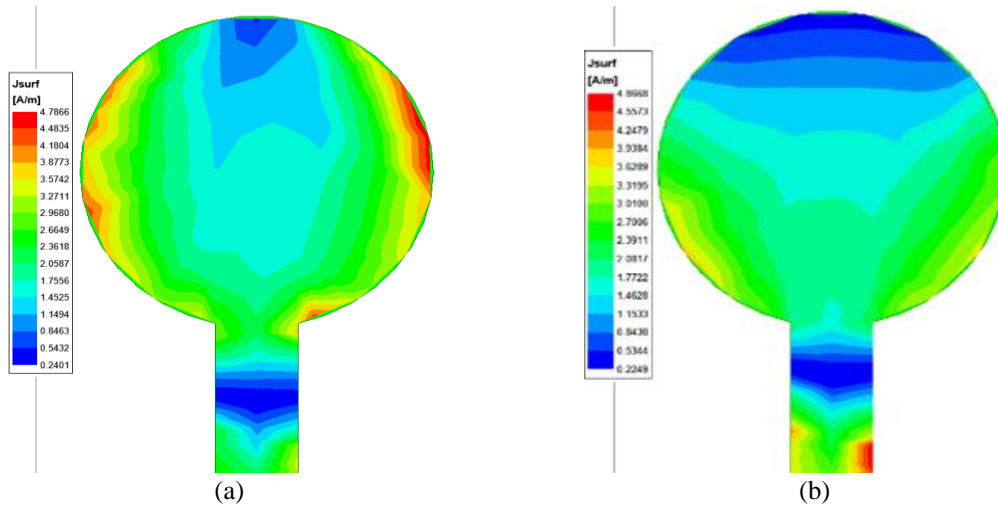


Figure 6. Current distribution, (a) at 28.1575 GHz and (b) at 38.5625 GHz

The comparison has shown that our design provided excellent performance metrics in terms of bandwidth, gain, and miniaturization. The bandwidth dimensions ratio (BDR) is an additional performance index that measures the miniaturization and the wide bandwidth. The BDR is computed by (4) [24]. A large BDR indicates that the antenna has miniaturized dimensions and wider bandwidth. From Table 3, it can be observed that our proposed work has a larger BDR value. Thus, the proposed SR-DGS antenna is more miniaturized since it has more bandwidth per unit area. This makes it one of the best-suited designs for 5G applications since the antenna can be easily integrated into space-constrained devices.

$$BDR = \frac{BW (\%)}{\lambda_{length} \times \lambda_{width}} \tag{4}$$

BW (%) is the fractional bandwidth, λ_{length} and λ_{width} are the proposed antenna’s electrical length and width corresponding to the lower end operating frequency that meets the -10 dB reflection coefficient or $VSWR < 2$.

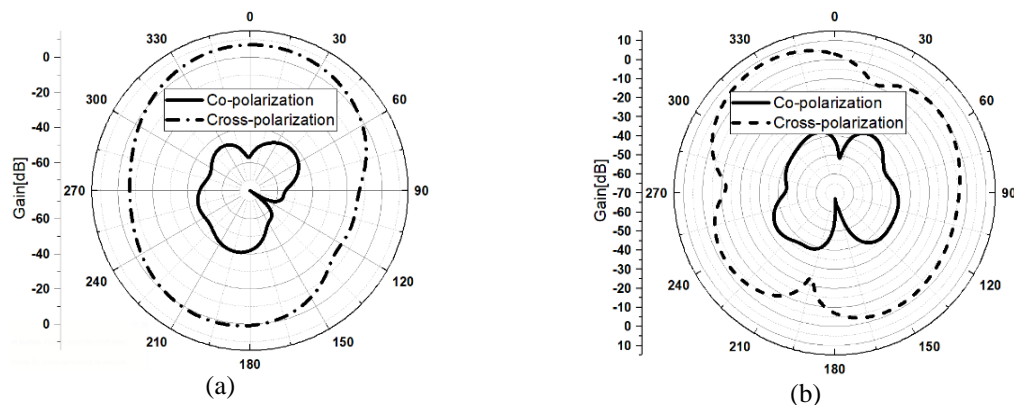


Figure 7. E-plane patterns, (a) 28 GHz and (b) 38 GHz

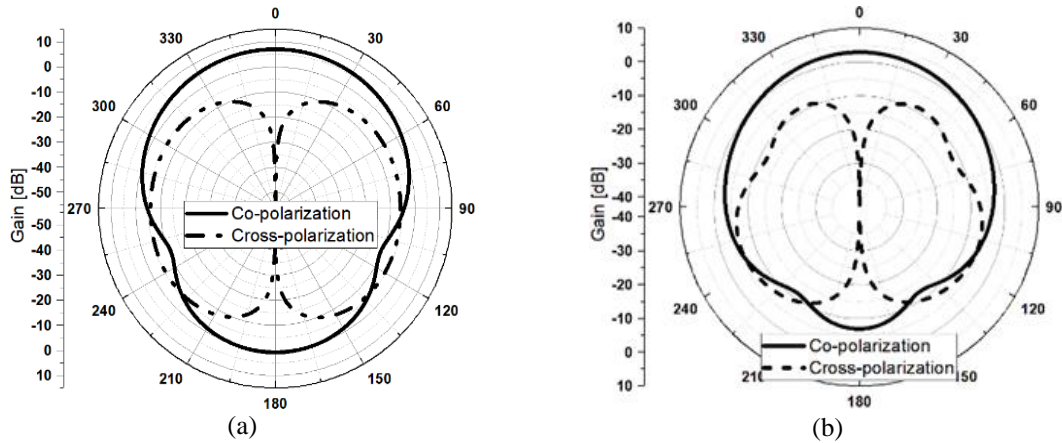


Figure 8. H-plane patterns, (a) 28 GHz and (b) 38 GHz

Table 3. Comparison of the proposed design with other works in the open literature

Ref.	Freq. Bands	Bandwidth [GHz]	Gain [dB]	VSWR	Electrical size	BDR
Colaco and Lohani [4]	26 GHz	3.56	10	1.03	$0.29\lambda_0 \times 0.39\lambda_0 \times 0.056\lambda_0$	5.4
Qayyum <i>et al.</i> [15]	28 GHz	0.87 GHz	6.87 dBi	Not given	$0.667\lambda_0 \times 0.667\lambda_0 \times 0.0544\lambda_0$	6.968
Gupta and Bage [16]	28 GHz	0.7 GHz	8.21	Not given	$1.12\lambda_0 \times 1.31\lambda_0 \times 0.035\lambda_0$	1.7
	38 GHz	0.5 GHz	5.74			
Nahas [20]	26 GHz	0.55 GHz	8.63	1.13	$1.7\lambda_0 \times 1.41\lambda_0 \times 0.044\lambda_0$	0.884
	28 GHz	1.1 GHz	11.26	1.11		
Lodro <i>et al.</i> [25]	37 GHz	5.5	5.5	Not given	$0.86\lambda_0 \times 0.6\lambda_0 \times 0.094\lambda_0$	27.5
	54 GHz	8.67	6			
Darboe <i>et al.</i> [26]	28 GHz	0.847	6.63	1.5376	$0.577\lambda_0 \times 0.664\lambda_0 \times 0.0459$	7.882
Mungur <i>et al.</i> [27]	28 GHz	0.582	6.69	1.77	$0.31\lambda_0 \times 0.377\lambda_0 \times 0.025\lambda_0$	17.90
Asgar <i>et al.</i> [28]	67GHz (64.8-69)	4.2	8.9	<1.5	$1.19\lambda_0 \times 1.017\lambda_0 \times 0.082\lambda_0$	5.12
Teresa and Umamaheswari [29]	28 GHz	2.62	6.59	1.08	$0.626\lambda_0 \times 0.626\lambda_0 \times 0.07\lambda_0$	23.73
El-Sayed <i>et al.</i> [30]	17.07 GHz	0.810	7.65	Not given	$1.21\lambda_0 \times 1.21\lambda_0 \times 0.044\lambda_0$	3.238
	26.82 GHz	0.845	5.64			
This Work	28 GHz	1.34	7.19	1.0175	$0.458\lambda_0 \times 0.366\lambda_0 \times 0.144\lambda_0$	28.34
	38 GHz	2.26	7.61	1.0580		

4. CONCLUSION

This article investigates a unique miniaturized microstrip antenna for 5G mobile networks. The suggested antenna has a physical overall dimension of $5 \times 4 \times 1.575 \text{ mm}^3$ and an electrical overall size of $0.458\lambda_0 \times 0.366\lambda_0 \times 0.144\lambda_0$; λ_0 denotes the free space wavelength at 27.50 GHz. The patch area of 9.19 mm^2 demonstrates the compactness of the proposed radiator. The result has shown -10 dB impedance bandwidths of 1.34 GHz (27.50 GHz-28.84 GHz) and 2.26 GHz (37.74 GHz-40 GHz) at the 28 and 38 GHz bands, respectively. In terms of radiation, the antenna exhibits quasi-omnidirectional radiation patterns with maximum gains of 7.2 dB and 7.65 dB, at the two resonant frequencies, respectively. The radiation efficiency of the antenna is 94% in the entire frequency range. Reflection coefficients of -38.3 dB and -30.8 dB are achieved at the respective resonant frequencies with corresponding VSWR values of 1.0175 and 1.0580. Considering the mentioned key performance indexes, our proposed SR-DGS antenna is one of the most suitable candidates for 5G communication systems. For future work, the performance of the proposed single element antenna can be improved by developing the antenna into a multiple input multiple output (MIMO) antenna for 5G networks.

ACKNOWLEDGEMENTS

The authors would like to appreciate the African Union Commission (AUC) for funding this research activity. They also acknowledge the support from the administration of the Pan African University, Institute for basic Sciences, Technology and Innovation (PAUSTI), including all lecturers and staff. Finally, they extend their thanks to Dr. Pierre Mukala Mpele for his technical assistance.




REFERENCES

- [1] R. Chataut and R. Akl, "Massive MIMO systems for 5G and beyond networks-overview, recent trends, challenges, and future research direction," *Sensors (Switzerland)*, vol. 20, no. 10, pp. 1–35, 2020, doi: 10.3390/s20102753.
- [2] R. Przesmycki, M. Bugaj, and L. Nowosielski, "Broadband microstrip antenna for 5G wireless systems operating at 28 GHz," *Electron.*, vol. 10, no. 1, pp. 1–19, 2021, doi: 10.3390/electronics10010001.
- [3] P. M. Mpele, F. M. Mbango, D. B. O. Konditi, and F. Ndagijimana, "A tri-band and miniaturized planar antenna based on countersink and defected ground structure techniques," *Int. J. RF Microw. Comput. Eng.*, vol. 31, no. 5, pp. 1–12, 2021, doi: 10.1002/mmce.22617.
- [4] J. Colaco and R. Lohani, "Design and implementation of microstrip patch antenna for 5G applications," no. June, pp. 682–685, 2020, doi: 10.1109/icc48766.2020.9137921.
- [5] A. B. Sahoo, N. Patnaik, A. Ravi, S. Behera, and B. B. Mangaraj, "Design of a miniaturized circular microstrip patch antenna for 5G applications," *Int. Conf. Emerg. Trends Inf. Technol. Eng. ic-ETITE 2020*, pp. 3–6, 2020, doi: 10.1109/ic-ETITE47903.2020.374.
- [6] S. E. Dyasti, M. M. Mostafa, H. Ghaz, and M. F. A. Sree, "Novel and compact circular ring microstrip antenna with parasitic chip for 5G applications," *J. Phys. Conf. Ser.*, vol. 2128, no. 1, 2021, doi: 10.1088/1742-6596/2128/1/012007.
- [7] M. A. Jiddney, M. Z. Mahmud, M. Rahman, L. C. Paul, and M. T. Islam, "A circular shaped microstrip line fed miniaturized patch antenna for 5G applications," *2020 2nd Int. Conf. Sustain. Technol. Ind. 4.0, STI 2020*, vol. 0, pp. 19–20, 2020, doi: 10.1109/STI50764.2020.9350513.
- [8] C. L. Bamy, F. M. Mbango, D. B. O. Konditi, and P. M. Mpele, "A compact dual-band Dolly-shaped antenna with parasitic elements for automotive radar and 5G applications," *Heliyon*, vol. 7, no. 4, p. e06793, 2021, doi: 10.1016/j.heliyon.2021.e06793.
- [9] C. L. Bamy, and P. M. Mpele, "Asymmetric-fed triband antenna for military radars and 5G applications using microstrip technology," *The Journal of Engineering*, 2022.
- [10] S. Kumar and A. Kumar, "Design of circular patch antennas for 5G applications," *Proc. 2nd Int. Conf. Innov. Electron. Signal Process. Commun. IESC 2019*, pp. 287–289, 2019, doi: 10.1109/IESPC.2019.8902384.
- [11] R. Ruchi and P. Upadhyaya, "5G antenna at millimeter wave frequency," *IEEE International Conference on Advances in Computing, Communication Control and Networking*, no. December, 2021, doi: 10.1109/ICAC3N53548.2021.9725701.
- [12] A. F. Kaeib, N. M. Shebani, and A. R. Zarek, "Design and analysis of a slotted microstrip antenna for 5G communication networks at 28 GHz," *19th Int. Conf. Sci. Tech. Autom. Control Comput. Eng. STA 2019*, pp. 648–653, 2019, doi: 10.1109/STA.2019.8717292.
- [13] K. A. Fante and M. T. Gameda, "Broadband microstrip patch antenna at 28 GHz for 5G wireless applications," *Int. J. Electr. Comput. Eng.*, vol. 11, no. 3, pp. 2238–2244, 2021, doi: 10.11591/ijece.v11i3.pp2238-2244.
- [14] L. C. Paul, M. H. Ali, N. Sarker, M. Z. Mahmud, R. Azim, and M. T. Islam, "A wideband rectangular microstrip patch antenna with partial ground plane for 5G applications," *2021 Jt. 10th Int. Conf. Informatics, Electron. Vision, ICIEV 2021 2021 5th Int. Conf. Imaging, Vis. Pattern Recognition, icIVPR 2021*, no. October, 2021, doi: 10.1109/ICIEVICIVPR52578.2021.9564160.
- [15] A. Qayyum, A. H. Khan, S. Uddin, O. Ahmad, J. S. Khan, and S. Bashir, "A novel mmwave defected ground structure based microstrip antenna for 5G cellular applications," *Proc. - 2020 1st Int. Conf. Smart Syst. Emerg. Technol. SMART-TECH 2020*, pp. 28–31, 2020, doi: 10.1109/SMART-TECH49988.2020.00023.
- [16] S. K. Gupta and A. Bage, "A compact, dual-band antenna with defected ground structure for 5G applications," *J. Circuits, Syst. Comput.*, vol. 30, no. 16, 2021, doi: 10.1142/S0218126621502984.
- [17] A. Kapoor, R. Mishra, and P. Kumar, "Wideband miniaturized patch radiator for Sub-6 GHz 5G devices," *Heliyon*, vol. 7, no. 9, p. e07931, 2021, doi: 10.1016/j.heliyon.2021.e07931.
- [18] A. N. D. Ghz, P. Antenna, and M. M. M. Omar, "Sensors," 2020.
- [19] M. Hussain *et al.*, "Design and fabrication of a printed tri-band antenna for 5g applications operating across ka-, and v-band spectrums," *Electron.*, vol. 10, no. 21, pp. 1–10, 2021, doi: 10.3390/electronics10212674.
- [20] M. Nahas, "A super high gain l-slotted microstrip patch antenna for 5G mobile systems operating at 26 and 28 GHz," *Eng. Technol. Appl. Sci. Res.*, vol. 12, no. 1, pp. 8053–8057, 2022, doi: 10.48084/etasr.4657.
- [21] P. M. Mpele, F. M. Mbango, and D. B. O. Konditi, "A small dual band (28/38ghz) elliptical antenna for 5g applications with dgs," *Int. J. Sci. Technol. Res.*, vol. 8, no. 10, pp. 353–357, 2019.
- [22] M. I. Khattak, A. Sohail, U. Khan, Z. Ullah, and G. Witjaksomo, "Elliptical slot circular patch antenna array with dual band behaviour for future 5G mobile communication networks," *Prog. Electromagn. Res. C*, vol. 89, no. January, pp. 133–147, 2019, doi: 10.2528/PIERC18101401.
- [23] P. K. Malik, S. Padmanaban, and J. B. Holm-Nielsen, "Microstrip antenna design for wireless applications," *New York: CRC Press*, 2022.
- [24] W. Balani, M. Sarvagya, A. Samasgikar, T. Ali, and P. Kumar, "Design and analysis of super wideband antenna for microwave applications," *Sensors (Switzerland)*, vol. 21, no. 2, pp. 1–29, 2021, doi: 10.3390/s21020477.
- [25] Z. Lodro, N. Shah, E. Mahar, S. B. Tirmizi, and M. Lodro, "MmWave novel multiband microstrip patch antenna design for 5G communication," *2019 2nd Int. Conf. Comput. Math. Eng. Technol. iCoMET 2019*, pp. 1–4, 2019, doi: 10.1109/ICOMET.2019.8673447.
- [26] O. Darboe, D. B. O. Konditi, and F. Manene, "A 28 GHz rectangular microstrip patch antenna for 5G applications," *Int. J. Eng. Res. Technol.*, vol. 12, no. 6, pp. 854–857, 2019.
- [27] S. Mungur, D. Duraikannan, "Microstrip patch antenna at 28 GHz for 5G applications," *J. Sci. Technol. Eng. Manag. Res. Innov.*, vol. 1, no. 1, pp. 20–22, 2018.
- [28] M. Asghar, S. Lupin, S. Shoaib, and P. Excell, "Design and analysis of compact antenna for 5G communication devices," *Proc. 2020 IEEE Conf. Russ. Young Res. Electr. Electron. Eng. EICoN Rus 2020*, pp. 2236–2239, 2020, doi: 10.1109/EICoN Rus49466.2020.9039525.
- [29] P. M. Teresa and G. Umamaheswari, "Compact slotted microstrip antenna for 5G applications operating at 28 GHz," *IETE J. Res.*, no. October, 2020, doi: 10.1080/03772063.2020.1779620.
- [30] M. El-Sayed, N. Gad, M. El-Aasser, and A. Yahia, "Slotted rectangular microstrip-antenna design for radar and 5 G applications," *Proc. 2020 Int. Conf. Innov. Trends Commun. Comput. Eng. ITCE 2020*, no. February, pp. 330–334, 2020, doi: 10.1109/ITCE48509.2020.9047754.




BIOGRAPHIES OF AUTHORS

Mamadou Mamarou Diallo    is a research student who is currently pursuing a Master's degree at the Pan African University, Institute for basic Sciences, Technology and Innovation (PAUSTI), Kenya. He received the BSc degree in Electronics Engineering (Telecommunication Networks) from the University Gamal Abdel Nasser of Conakry (UGANC), Guinea. His research interest includes RF and Microwave components design, Communication systems, and future wireless communication standards. He can be contacted at email: mamarou.mamadou@students.jkuat.ac.ke.



Dominic Bernard Onyango Konditi    is a professor of electrical and electronic engineering at Technical University of Kenya (TU-K). He received his PhD in Electronics and Computer Engineering from IIT Roorkee, INDIA, MSc-Engineering in Electrical and Communication Engineering from Tottori University, JAPAN, and Postdoc Res. from Dresden University of Technology (DUT), Germany. Professor's research interests are in design and modelling smart antennas, analysis and modelling radiowave propagation problems, modelling electromagnetic compatibility and electromagnetic interference problems. He has taught and supervised at postgraduate level. He has also published extensively in reputable journals and refereed conference proceedings. He can be contacted at email: dominic.konditi@tukenya.ac.ke.



Olivier videme Bossou    Got his PhD in Electromagnetism from Ecole Polytechnique Fédéral de Lausanne (EPFL) in Switzerland. He is currently an Associate Professor at the National Advanced School of Engineering of Yaoundé at the University of Yaoundé-1. His main research interests include antennas, electromagnetism, microwaves and Telecommunication engineering. He can be contacted at email: bossou.videme@univ-yaounde1.com.